A video technique for the quantitative analysis of the Poisson spot and other diffraction patterns

G. Robert Wein
Department of Physics, Southern Connecticut State University, New Haven, Connecticut 06515

(Received 22 September 1997; accepted 20 July 1998)

A new approach is presented for the observation and analysis of diffraction phenomena. Using the discussed procedures, direct comparison between measured light intensity and theoretical predictions is possible. A modified version of a Poisson spot experiment where the resulting diffraction pattern is recorded by a Sanyo vidicon camera is presented. A double slit experiment is also discussed, demonstrating the quantitative possibilities while addressing detector linearity. A video signal is connected directly to a computer and analyzed using public domain software. This is an excellent arrangement for demonstrations, student labs, or a more general diffraction experiment. © *1999 American Association of Physics Teachers.*

I. INTRODUCTION

When students begin the study of optics and light, the existence of the Poisson spot is offered as evidence of the wave nature of light. Recent work with the spot has updated the experiment for demonstration purposes.[1,2] Modern physics topics can now be introduced using neutron and electron diffraction to produce the spot.[3,4]

Also presented to all physics students is Young's double slit experiment. Theoretical results can be derived, and for corroboration, the fringe spacing of a distant pattern is measured. Missing fringes are easily explained as the zero points of the derived envelope function. Unfortunately this explanation leads to the additional result that partially obscured fringes had their centers apparently shifted, therefore limiting the fringe spacing measurement reliability.

To anticipate the diffraction effects in an optical system, one is required to recall the theoretical calculations, use computer software, or search for previously reported similar results. Even for the simplest cases experimenters are often limited to the photographs presented in textbooks.[5–8] The utility of those photographic images is, in turn, limited by the film's nonlinearity and dynamic range.

Theoretical analysis has become more accessible with the existence of software such as DAFRAC.[9] However, typical numerical solutions of the diffraction theory integrals do not provide for the intermediate field case, where the pattern is still qualitatively changing. Moreover, solving the relevant equations at a set distance can promote the impression that a diffraction pattern is similar to a real image found in geometrical optics: two dimensional and located at a fixed point. Not only does a diffraction pattern exist at all points along the optical axis, there are also qualitative changes in its structure and quantitative changes in its intensity profile. This paper will discuss a simple and inexpensive method for measuring the qualitative and quantitative changes in diffraction patterns at different points along the optical axis using the Poisson spot and Young's double slit experiments as examples.

II. THE POISSON SPOT EXPERIMENT

Figure 1 shows the experimental apparatus. The laser used in the present experiment was a Melles Griot 1.5-mW, 543.5-nm helium–neon with random polarization. The output diameter of the beam was specified as 0.8 mm with a 0.81-mrad divergence angle. Other laser beams, including a 670-nm laser "pointer," were also used with similar success; however, all results presented here were obtained with the green HeNe laser.

The beam diameter was increased by using an expander made with two plano-convex lenses. The lenses were separated by the sum of their focal lengths and the net magnification was approximately ten. This had the added benefit of reducing the beam's divergence.

To improve the beam's intensity profile, a spatial filter was placed near the shared focal point of the two lenses in the beam expander. A 40-μm pinhole was mounted on an $x-y-z$ translation stage. It was placed at approximately the center of the beam, then adjusted to maximize the transmitted light. Spurious diffraction effects caused by dust or scratches before the spatial filter were lost as the beam passed through the pinhole.

To characterize the beam profile, a laser beam analyser, Spiricon model LBA-100, and a research grade Cohu charge-coupled device (CCD) camera were used. The central 6 mm of the beam fit a Gaussian profile with a correlation of 0.9 or better.

The obstacle, a 4.59-mm steel ball bearing, was chosen because it had a diameter slightly smaller than the narrower dimension of the rectangular video detectors (the standard 2/3-in. format is 8.8 by 6.6 mm). In addition a ball of this size is easy to cement in place without introducing spurious effects. The ball bearing was cemented to a 4-cm 60° prism approximately 1 cm from a vertex. This method of suspension avoids the additional fringes that could appear if a microscope slide or a narrow magnetized pin were used. A prism of this shape has the additional benefit of not magnifying the beam along one axis. If the beam is incident normal to the first surface, it is totally internally reflected, exiting perpendicular to the third face.

The prism was mounted on a rotational stage. A 120° rotation could then remove the ball from the beam, centering the now undiffracted beam on the camera, while preserving the optical path length in the prism. Thus any diffraction effects caused by optical elements other than the ball bearing could be recognized.

The video camera used was a black and white Sanyo vidicon model VCV 1500. For comparison, a research grade

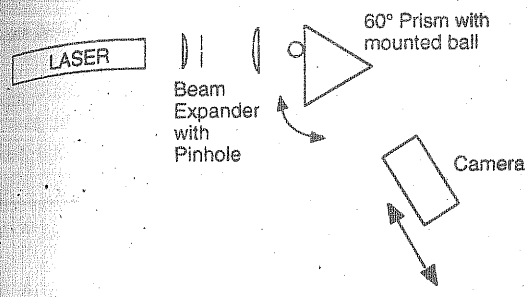

Fig. 1. A layout to display the Poisson spot (not to scale). This arrangement, with the camera mounted on a movable base, is effective for examining both near and far-field effects. The stray diffraction caused by objects other than the ball, or similar obstacle, can be subtracted by recording the beam intensity after a 120° rotation of the prism. The beam magnification was approximately 10×.

Cohu CCD camera was also used and this was found to provide no added benefit. For both cameras, the lenses were removed to prevent focusing the beam.

To record the diffraction pattern, the camera was directly connected to a Macintosh 8100/100 AV through the standard RCA connector. The program, NIH Image version 1.62 (written by Wayne Rasband at the U.S. National Institutes of Health and available from the internet by anonymous ftp from zippy.nimh.nih.gov[10] or on floppy disk from NTIS, 5285 Port Royal Rd., Springfield, VA 22161, part number PB93-504868) was used to display and analyze the data. It has the ability to average up to 4096 sequential images, draw cross-sectional plots and false color surface maps, and export numerical light intensity values for use in spreadsheets.

Calibrating the spatial resolution of the camera/Image program system allows distance measurements between features of the diffraction pattern at any point in space. Figure 2 is the

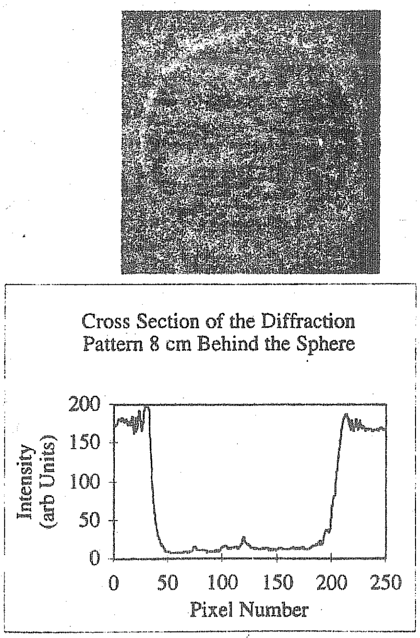

Fig. 2. The diffraction pattern as collected by the Sanyo video camera 8 cm behind the 4.59-mm steel ball bearing. The upper image, 220 pixels on a side, is the average of 100 frames, taking approximately 10 s. The plot shows an intensity profile, with the clearly evident Poisson spot.

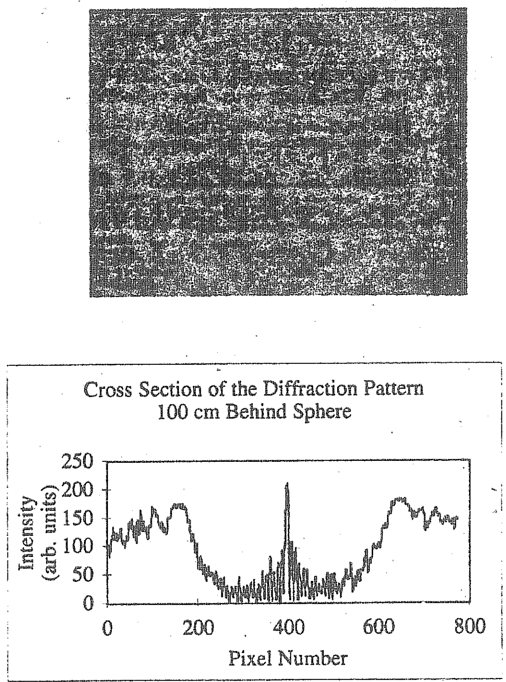

Fig. 3. The diffraction pattern as collected by the Sanyo video camera 100 cm behind the 4.59-mm steel ball bearing. The upper image is an average of 100 frames. The lower plot is a diagonal cross section showing the central spot and its surrounding concentric rings.

diffraction pattern as recorded by the Sanyo vidicon camera when the detector surface was 8 cm from the object plane. This was done with the smallest object image separation that yielded a clear Poisson spot, thus ensuring the smallest possible spot size. The trace beneath the pattern is an intensity profile along a diameter line. To calibrate the camera, a precision translation stage was used to displace the camera in a plane perpendicular to the optic axis. The number of pixels the Poisson spot moved in the displayed image was counted. Dividing the distance moved, as measured by the translation stage micrometer, by the pixel count gave an average of 13.72 μm/pixel.

III. POISSON SPOT RESULTS AND ANALYSIS

An image of the diffraction pattern was recorded every 10 cm as the object to detector distance was varied from 10 to 200 cm. Each image was the average of 100 frames, and took approximately 10 s to create. All frames are clear, free of spurious effects and offer 8-bit greyscale resolution. Figures 3 and 4 are two representative diffraction patterns recorded at object-image distances of 100 and 180 cm, respectively. While the spot is evident in both images, the distance between adjacent fringes increases. Using the cross-section tool within the NIH Image program, approximately 25 peak locations were recorded. The measured fringe spacing is 118.5 μm at 100 cm and 210.3 μm at 180 cm.

Apparent in Figs. 3 and 4 is the continuation of concentric rings from the geometric shadow region. Here they are dominated by the broader single-edge diffraction fringes. Looking at the intensity distribution in cross section, the superposition

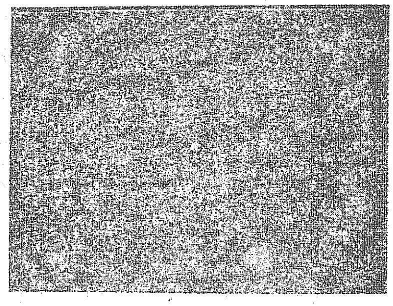

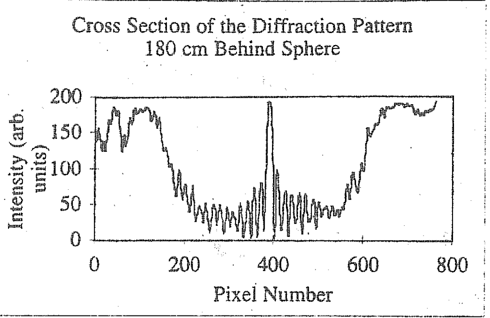

Fig. 4. This is the same as Fig. 3 except the image plane is 180 cm behind the ball bearing.

of the two different patterns is evident. Photographs of these patterns cannot show this much detail in both regions simultaneously.

The concentric rings within the geometric shadow region of the pattern are not superimposed on any other effect. Many high contrast fringes are clearly visible. This means that very accurate peak locations and separations can be obtained, unlike in Young's double slit.

The bright spot in the center of a ball's geometrical shadow and its interesting history are often discussed in optics texts.[11,12] More recent work has treated the problem quite elegantly,[13–15] including the rigorous solution of the appropriate Kirchhoff integrals.

The diffraction theory treatment, as outlined in Refs. 13–15, is quite helpful when generating light intensity plots. However, they do not offer a closed form solution to the following question: How far apart are the fringes? Figure 5 is

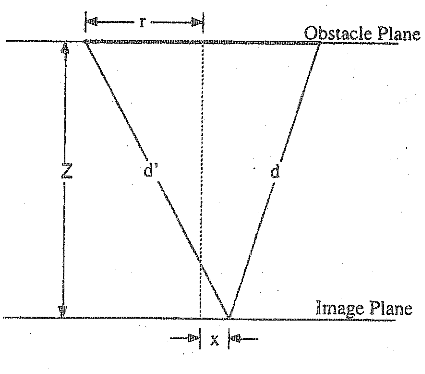

Fig. 5. The obstacle plane of the experiment is perpendicular to the optical axis and contains the center of the sphere of radius r. "Z" is the distance to the camera's detector surface. "x" is the position relative optical axis. while d and d' are measured from the sphere's edges to that same point.

a ray diagram of the object to image plane region and shows that

$$(r+x)^2+z^2=d'^2 \tag{1a}$$

$$(r-x)^2+z^2=d^2. \tag{1b}$$

Solving these expressions for x yields

$$x=\frac{1}{4r}(d'^2-d^2). \tag{2}$$

The condition for constructive interference at some position in the image plane is just

$$d'-d=n\lambda. \tag{3}$$

If the approximation is made that $d+d'=2z$, the expression for the location of concentric rings of maximum intensity is $x=n\lambda z/2r$. The separation between successive maxima is therefore

$$\Delta x=\lambda z/2r. \tag{4}$$

The Appendix examines the effects of relaxing the above approximation.

It should be recognized that implicit in this result is the treatment of the diffracting wave fronts as diametrically opposed point sources at the edge of the obstacle. This is consistent with the Huygens–Fresnel principle[16] and the half-period zone construction in Jenkins and White.[17] The amplitude from the first exposed half-period zone has twice the resultant amplitude from all the remaining zones.[18] Therefore, because of the diminishing contributions from successive zones, it is assumed that the fringe maxima are at the positions predicted when considering the first exposed zone by itself. The width of the first exposed zone calculates to 0.1 mm, so it is approximated as a ring of point sources. Furthermore the symmetry of the experiment suggests that off-axis contributions do not affect peak positions. This is analogous to a rectangular opening's fringe spacing along one axis not being affected by the perpendicular dimension.[19]

To examine the validity of this approach, Eq. (4) was used to calculate the diameter of the ball. A very good agreement was achieved in both cases: 4.58 and 4.65 mm at 100 and 180 cm, respectively. The accuracy of 1% is presently limited by the ability to measure the ball-to-detector-plane separation. This could be improved by removing the detector from the camera body or using an inexpensive board mounted CCD camera.

To further check the above fringe spacing equation, the radius and separation appropriate for the experiment in Rinard's work[13] were used to calculate the fringe separation in that experiment. The results are in excellent agreement with his results, which were derived using the Kirchhoff integrals and the necessary Bessel and Lommel functions.

IV. DOUBLE SLIT EXPERIMENT

In addition to spatial measurements, the relative intensity within diffraction patterns is also of interest. To address this quantitatively, a detector's linearity needs to be verified. Recording the Young's double slit diffraction pattern and comparing the results to the theoretically predicted closed form solution allows for that determination. Many books directed toward the calculus-based introductory physics course include a discussion of the Fraunhofer, or far field, diffraction

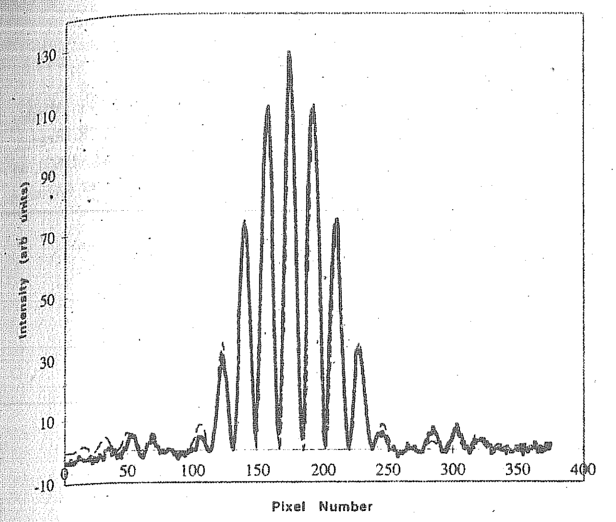

Fig. 6. The intensity of the double slit diffraction pattern as created using the layout of Fig. 1 and Ref. 16. The dashed line is the theoretical curve, generated using Eq. (5). The data, as recorded by a Sanyo vidicon camera, are shown as the solid line.

pattern of a double slit.[20] More advanced treatments found in optics textbooks offer complete intensity distribution derivations, assuming the screen is infinitely far away.[5,6,8] However, none of these provide a quantitative comparison of theory and experiment.

The familiar optical layout[21] for the double slit experiment employed a pair of 0.24-mm slits separated by 1.2 mm, supplied by Leybold. Illumination was provided by the same laser as in Sec. II, with the prism rotated 120°.

Figure 6 shows the resulting experimental diffraction pattern as recorded from the video camera with NIH Image providing the background subtraction. The cross-section tool of the Image program was used, as with the Poisson spot experiment, and the resulting intensity values were exported as a text file and plotted using Microsoft EXCEL. Superimposed in Fig. 6 is the standard far-field theoretical result,[22]

$$I=4I_0\,\frac{\sin^2\left[\dfrac{\pi b}{\lambda}\sin\left(\tan^{-1}\dfrac{x}{z}\right)\right]}{\left[\dfrac{\pi b}{\lambda}\sin\left(\tan^{-1}\dfrac{x}{z}\right)\right]^2}\cos^2\left[\frac{\pi a}{\lambda}\sin\left(\tan^{-1}\frac{x}{z}\right)\right]. \tag{5}$$

The theoretical curve was normalized to the experimental central maximum. The object-image separation "z" was measured as 0.55 m. The position within the pattern, as measured from the center, is "x," the pixel number multiplied by pixel width, 13.72 μm. Looking at Fig. 6, one can see that the agreement between theory and experiment is excellent. This suggests that the response of the detector is linear over its entire range and relative intensity measurements can therefore be made with this arrangement. For instance, covering one of the slits produces a drop in central intensity by a factor of 4.

V. CONCLUSIONS

A simple geometry has been suggested for imaging the Poisson spot. It is inexpensive and eliminates many of the spurious effects apparent in other arrangements. It is even possible to change the ball or remove it from the expanded laser beam without changing the optical path.

It has been shown that the ball diameter is accurately measured using a constructive interference model in the geometrical shadow region. This has implications for the measurement of objects not as simple as steel balls. For instance the diameter of bubbles or imbedded defects in polymers could be measured very rapidly.

The possibility for excellent undergraduate optics experiments was demonstrated. This quantitative analysis successfully bridges the gap between the typical Young's double slit experiment of introductory physics and the theoretical results developed in an advanced optics course. By moving the camera along the optical axis in either experiment, the three-dimensional nature of the diffraction pattern is readily apparent. The wave property of light is rapidly displayed, and true quantitative measurements are straightforward.

ACKNOWLEDGMENTS

This work was supported by a Connecticut State University Faculty Research Grant. Valuable assistance with the equipment was provided by Eric Anderson. Spiricon's donation of a model LBA-100 laser beam analyzer was most helpful.

APPENDIX

If Eqs. (1a) and (1b) are solved for d' and d, we have

$$d'=\sqrt{(r+x)^2+z^2}=z\left[1+\left(\frac{r+x}{z}\right)^2\right]^{1/2}, \tag{A1A}$$

$$d=\sqrt{(r-x)^2+z^2}=z\left[1+\left(\frac{r-x}{z}\right)^2\right]^{1/2}. \tag{A1B}$$

Expanding the radicals, keeping the first three orders, and subtracting yields

$$d'-d=n\lambda=\frac{rx}{z}\left[2-\left(\frac{r^2+x^2}{z^2}\right)\right]. \tag{A2}$$

The first term is identical to Eq. (4). The second term in the brackets is of the order 0.001 for the present experiment, and is therefore considered negligibly small when compared to possible experimental error.

[1]M. E. Harrison, C. T. Marek, and J. D. White, "Rediscovering Poisson's Spot," Phys. Teach. **35**, 18–19 (1997).

[2]J. Higbie, "More on Poisson's Spot," Phys. Teach. **35**, 197 (1997); R. D. Wong, "Still More on Poisson's Spot," *ibid.* **35**, 197–198 (1997).

[3]R. Gahler and A. Zeilinger, "Wave-optical experiments with very cold neutrons," Am. J. Phys. **59** (4), 316–324 (1991).

[4]G. Matteucci, "Electron wavelike behavior: A historical and experimental introduction," Am. J. Phys. **58** (12), 1143–1147 (1990).

[5]F. L. Pedrotti and L. S. Pedrotti, *Introduction to Optics* (Prentice-Hall, Englewood Cliffs, NJ, 1993), 2nd ed.

[6]J. R. Meyer-Arendt, *Introduction to Classical and Modern Optics* (Prentice–Hall, Englewood Cliffs, NJ, 1995), 4th ed.

[7]M. Cagnet, M. Francon, and J. C. Thrierr, *Atlas of Optical Phenomena* (Springer-Verlag, Berlin, 1962).

[8]F. A. Jenkins and H. E. White, *Fundamentals of Optics* (McGraw–Hill, New York, 1976), 4th ed.

[9]DAFRAC, a program written by G. Forbes and P. Hoch, available from the Optical Society of America, Customer Service, 2010 Massachusetts Avenue NW, Washington, DC 20036–1023.

[10]Anonymous ftp site for NIH Image program: zippy.nimh.nih.gov

[11] R. A. Houstoun, *A Treatise on Light* (Longmans, Green London, 1946), 7th ed., 164.

[12] J. W. Goodman, *Introduction to Fourier Optics* (McGraw–Hill, New York, 1996), 2nd ed.

[13] P. M. Rinard, "Large-scale diffraction patterns from circular objects," Am. J. Phys. **44** (1), 70–76 (1976).

[14] E. A. Hovenac, "Fresnel diffraction by spherical obstacles," Am. J. Phys. **57** (1), 79–84 (1989).

[15] J. A. Lock and E. A. Hovenac, "Diffraction of a Gaussian beam by a spherical obstacle," Am. J. Phys. **61** (8), 698–707 (1993).

[16] E. Hecht, *Optics* (Addison–Wesley, Reading, MA, 1998), 3rd ed., p. 434.

[17] See Ref. 8, p. 380.

[18] See Ref. 8, p. 384.

[19] See Ref. 8, p. 324.

[20] See, for example, H. D. Young, *University Physics* (Addison–Wesley, Reading, MA, 1992), 8th ed., pp. 1047–1054; D. Halliday, R. Resnick, and J. Walker, *Fundamentals of Physics* (Wiley, New York, 1993), 4th ed., pp. 1085–1087; R. A. Serway, *Physics for Scientists and Engineers* (Saunders, Philadelphia, 1996), 4th ed., pp. 1092–1098.

[21] See Ref. 16, p. 448.

[22] See Ref. 5, p. 339 or Ref. 16, p. 449.

KINES AND SPOUDS

The Velocity of a moving body may be stated in units of length per unit of time, *e.g.*, feet per second; and a body is moving with Unit velocity when it moves one foot per second, or one centimetre per second (the latter, the C.G.S. unit, being one '*Kine*'). It will be observed that it is necessary for us to make consistent use of the British or of the C.G.S. units of measurement and not to use them confusedly within the limits of the same problem. ...

A body, then, which has its velocity in a given direction increased or diminished by one foot in one second, two feet in two seconds, and so forth, is undergoing, in that direction, a unit acceleration, in British units; if by one cm. per sec., n cm. in n seconds, it is undergoing a unit acceleration (one '*Spoud*') in C.G.S. units.

Alfred Daniell, *A Text Book of the Principles of Physics* (Macmillan Company, London, 1911), pp. 14 and 18.